17th Brazilian Congress of Thermal Sciences and Engineering
November 25th-28th, 2018, Águas de Lindóia, SP, Brazil

ENCIT-2018-0063
NUMERICAL ANALYSIS OF COOLING OF ELECTRONIC COMPONENTS BY HEATSINKS WITH MICROCHANNELS

Felipe Guahyba dos Reis
Francis Henrique Ramos França
Leonardo Brito Kothe
Universidade Federal do Rio Grande do Sul, R. Sarmento Leite 425, Porto Alegre, 90050-170, Brazil
felipe.reis@ufrgs.br, frfranca@mecanica.ufrgs.br, leonardo.kothe@ufrgs.br

Abstract. *This paper presents a numerical study on the performance of heatsinks with microchannels. For the validation of the numerical tool, a comparison with a known experimental study is carried out, and then improvements available in the literature on the subject are tested and compared. The numerical simulations are performed with the Fluent® software using the Finite Volumes Method (FVM). The mesh quality is evaluated through the GCI (Grid Convergence Index) method. The numerical result of the thermal resistance of the heatsink from the experimental study on which the first part of this paper is based was 0.097 °C/W, whereas the experimental result was 0.090 °C/W (with a maximum temperature of 373 K), representing a difference of 7.2%. An improvement is performed by integrating the heatsink to a HVAC (heating, ventilation and air conditioning) system, which lowers the inlet temperature and consequently lowers the highest temperature found in the system (350 K for the same dissipated power) without changing the thermal resistance, but providing gains in reliability. Changes in the heatsink geometry are presented by decreasing the inlet area, causing the resistance to vary from 0.097 °C/W for the original channel to 0.272 °C/W for the channel that has the lowest height. A heatsink whose microchannels have waves in their longitudinal dimensions is shown, but the expected effects of better mixing and greater contact area for the heat flux were not observed for the boundary conditions of the original experiment, the calculated thermal resistance was of 0.102 °C/W. The last analysis presents an idealization where the heat flux is evenly distributed in the silicon volume, with a thermal resistance of 0.084 °C/W.*

Keywords: *Heatsinks; Heat Exchangers; Microchannels; Numerical study; Thermal Resistance*

1. INTRODUCTION

Electronic equipment has made its way into practically every aspect of modern life, from toys and appliances to high-power computers. Continued miniaturization of electronic systems has resulted in an increase in the amount of heat generated per volume. Unless properly designed and controlled, high rates of heat generation result in high operating temperatures for electronic equipment, which jeopardizes its safety and reliability. The failure rate of electronic equipment increases exponentially with temperature. Furthermore, the high thermal stresses in the solder joints of electronic components mounted on circuit boards resulting from temperature variations are the main causes of failure. Therefore, thermal control has become important in the design and operation of electronic equipment (Cengel, 2007). Liquid cooling technology is expected to achieve heat dissipation rates of up to 10 MW/m² (1000 W/cm²) with microchannels.

Kandlikar et al. (2003) and Kandlikar, (2005) carried out researches that cover topics such as a concise study on potential improvements in a system using heatsinks with microchannels to remove high heat fluxes, as well as studies on the evolution of the use of heat exchangers with smaller channels - taking into account the associated performance and manufacturing technology.

Numerical papers on CFD for heatsinks with microchannels provide insights into discretization approaches and resolution of different types of microchannels. Thakre et al., 2016, performed a numerical analysis of a straight microchannel very similar to that of Tuckerman and Pease, 1981, and its discretization as a single microchannel serves as the basis for the discretization of the present work model. Chein and Chen, 2009, studied the effect of different arrangements for the inlet and outlet of fluid in the microchannels, which assisted in the modeling of the inlets and outlets of the studied heatsink.

Kumar and Zunaid (2016) presented a CFD study on wavy microchannels. Wavy channels, wavy channels with obstructions and straight channels were compared - the Reynolds number was also varied. From this work it is possible to understand and model a wavy microchannel.

2. METHODOLOGY

In the experiment by Tuckerman and Pease, (1981), several heatsinks were manufactured and tested. Figure 1 shows a diagram of the basic heatsink. In a series of experiments, 50 μm wide channels with 50 μm walls were etched vertically using KOH (an orientation-dependent etching) (Kays *et al.*, 1964) to a depth of 300 μm in silicon with 400 μm thickness. A Pyrex® (borosilicate glass) cover plate was anodically bonded (Wallis *et al.*, 1969) over the channels and over a pair of etched manifolds at the ends of the channel array.

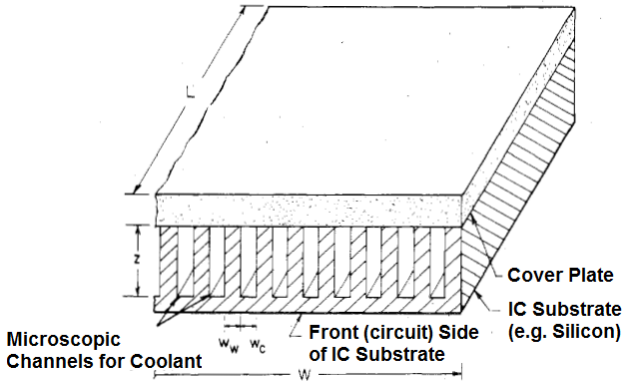

Figure 1 - Schematic view of a compact heatsink that uses microchannels built into an integrated circuit chip. [Adapted from Tuckerman and Pease, 1981]

Deionized water at approximately 23 °C was fed into the inlet manifold with pressures up to 0.214 N/mm². Heat was supplied by a WSi^2 thin film resistor with approximately 1 cm × 1 cm in area and 1 μm in thickness, which was positioned on the lower surface of the silicon wafer.

The performance of a heatsink is measured by its thermal resistance θ (Equation 1), where ΔT is the circuit temperature rise above the inlet temperature and $\dot{Q}$ is the dissipated power. Since semiconductor ICs typically have a maximum operating temperature of ΔT_{max} = 50 °C to 100° C above room temperature, the thermal resistance determines the maximum power at which an IC can operate. In general, θ is the sum of three components: θ_{cond}, due to the conduction through the substrate, encapsulation and interface with the heatsink; θ_{conv}, due to the convection of the heatsink with the coolant and $\theta_{(heating)}$, due to the heating of the fluid while absorbing the energy passing through the heatsink.

$$\theta = \frac{\Delta T}{\dot{Q}} \tag{1}$$

Table 1 summarizes the results obtained for three different heatsinks with similar parameters; all of them obtained the maximum thermal resistance (downstream) of about 0.1 °C/W for an area of 1 cm². One device has been tested up to 790 W/cm². This work focuses on the third and most power dissipating experiment. The original article did not present a study on the uncertainties of the experiment.

Table 1. Comparison between experiments

Experiment	w_c (μm)	w_w (μm)	z (μm)	P (N/mm²)	$\dot{f}$ (cm³/s)	θ_{max} (°C/W)	$\ddot{Q}$ (W/cm²)
1	56	44	320	0.103	4.7	0.110	181
2	55	45	287	0.117	6.5	0.113	277
3	50	50	302	0.214	8.6	0.090	790

2.1 Numerical Methodology

The heatsink was simulated numerically using the finite volume method (FVM) built in the commercial software Fluent® to compare the experimental results and improve the system based on previous work. The FVM uses as its starting point the integral form of the conservation equation. The solution domain is divided into a finite number of contiguous control volumes (CV), and the conservation equation is applied to each CV. In the centroid of each CV, it is located a computational node, in which the values of the variables are calculated, being the values of the variables in the surfaces of the CV obtained by interpolation as a function of the nodal values (center of the CV). Volume and surface

integrals are approximated using appropriate quadrature formulas. As a result, we obtain an algebraic equation for each CV, in which the values of the variables in the analyzed node and in the neighbors appear.

2.2 Discretization of the Model

The heatsink shown in Figure 1 was simplified using the inherent symmetry of the design. Therefore, only one of the 100 microchannels of the physical model was modeled in computer-aided design software Solidworks®.

As the inlet and outlet regions are not clearly presented in the original 1981 Tuckerman and Pease article, new regions in the front and back are added to the discretized model for the inlet and outlet, respectively, of coolant.

2.3 Boundary Conditions

The heatsink with microchannels was modeled according to the specifications of the third experiment of Tuckerman and Pease (Table 1): a silicon wafer with thickness of 400 μm coupled to a resistor with negligible thickness for the model (1 μm). The chemically etched microchannel has a height of 302 μm and a width of 50 μm. Above the system a Pyrex® cover is bonded - material with good thermal insulation (thermal conductivity of 1.14 W/m.K). The outer walls are considered adiabatic - with the exception of the lower one, with 790 W/cm² of dissipated power. The heat exchanges between the resistor and the coolant (water) are multiplied by the number of channels of the original experiment (100 channels) to evaluate the results. Figure 2 shows a schematic representing the boundary conditions.

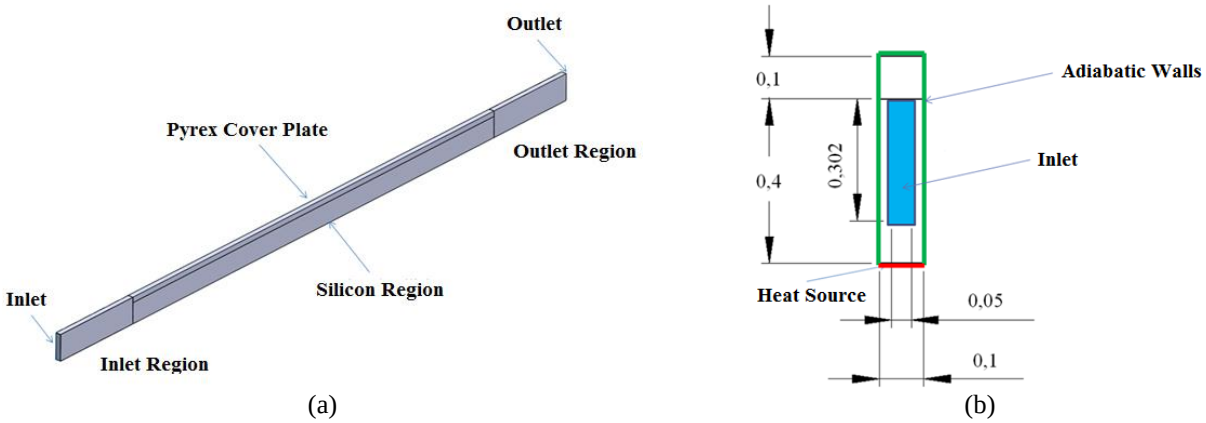

Figure 2. Schematic sketch of the boundaries: (a) isometric view; (b) front view.

2.4 Mesh Quality

As a mesh quality study, the GCI (Grid Convergence Index) method is chosen. Proposed by Roache, 1994, this method is based on Richardson's extrapolation and consists in a comparative of discrete solutions for different mesh sizes. This method was used in literature by Morais, 2004 and Oliveira, 2014. Three meshes (unstructured with tetrahedral volumes) of different sizes were created. Thus, simulations were performed to obtain the thermal resistance of the heatsink. For water with a pressure of 0.214 N / mm² at the inlet, a Reynolds number of 529 was found from the flow velocity of about 6.2 m/s. The values obtained for each mesh are shown in Table 2.

Table 2. Quantity of volumes of the three used meshes

Meshes	θ_{max} (°C/W)
Finer mesh (M1)	0.0974
Intermediate mesh (M2)	0.0957
Coarse mesh (M3)	0.0896

With the presented results, it is possible to calculate the asymptotic convergence value, reaching a value of 1.017. According to the method, for the solution to be within a range of convergence, the value must be closest to 1. With the results, it is also possible to estimate an "exact" solution value of 0.1032 °C/W. The obtained and calculated values can be seen in Table 3.

Table 3. Calculated values

Parameters	Values
$\theta_{max,exact}$ (estimated)	0.1032 °C/W
GCI_{12}	7.560%
GCI_{23}	9.871%
Value of asymptotic convergence	1.017

It was chosen the mesh with 1,053,165 volumes for the study, because it presents the best result and still has a computational time reasonable when compared to the coarser meshes.

3. RESULTS

In this chapter the numerical results are presented. The thermal resistance and maximum temperature of the studied heatsinks resulting from the computational simulations are presented.

3.1 Tuckerman and Pease Heatsink Numerical Results

By reproducing numerically the experiment of Tuckerman and Pease, 1981, it was possible to achieve a result very close to the experimental result (Figure 3(a), solid domain and Figure 3(b), fluid domain). With water at a pressure of 0.214 N/mm² and at a temperature of 296 K, a maximum temperature of about 373 K is reached in the system - a temperature variation of approximately 77 K. The heat transferred at the bottom of the heatsink is 790 W/cm², thus using Equation 1 a thermal resistance of 0.097 °C/W is reached (Table 4).

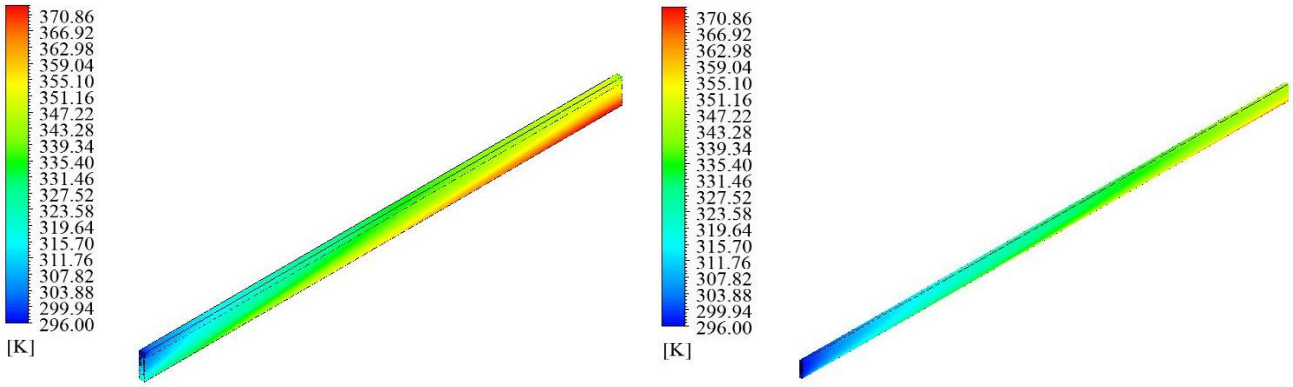

(a) (b)

Figure 3 - Temperature fields: (a) solid domain and (b) fluid.

Table 4. Comparison between numerical and experimental results for the heatsink of Tuckerman and Pease, 1981

	Experimental Result (°C/W)	Numerical Result (°C/W)	Difference (%)
Thermal Resistance	0.090	0.097	7.2

A difference of 7.2% between the experimental and numerical results indicates that the mesh and the used boundary conditions reproduce the problem reliably and that this tool can be used for the analysis and improvement of the heatsink, either in its geometry or in more favorable boundary conditions.

3.2 System Improvement - Integration with a Cooling System

Kandlikar, 2005, presented a way to increase the power that can be removed by the heatsink: by integrating it into a HVAC (heating, ventilation and air conditioning) system of a building, for example. In practice there is a decrease in the inlet temperature of the water, causing the maximum system temperature to be decreased.

By modifying the inlet temperature to 273 K and keeping the water at a pressure of 0.214 N/mm², the maximum temperature found in the system is about 350 K for the same power at the bottom of the heatsink (790 W/cm²). Thus, using Equation 1, the same thermal resistance of 0.097 °C/W is reached, since no geometric characteristics were altered.

However, the advantages of a lower maximum temperature are several, including a greater reliability of the system as a whole.

A further study was performed where the power is increased until the maximum system temperature is close to the original experiment so that gains from integrating the heatsink into a cooling system are fully appreciated. With a heat flux of 1000 W/cm² and an inlet temperature of 273 K a maximum system temperature of 371 K and the same maximum thermal resistance of 0.097 °C/W are reached.

3.3 Changes in Heatsink Geometry

3.3.1 Change in microchannel inlet geometry

Kandlikar, 2009, exploring what should be considered in the manufacture of heatsinks, cited that every aspect of the project has an associated cost, including channel depth, as more time is needed to reach greater depths. In this way, the effect of decreasing the channel depth in steps of 0.1 mm is studied, which will reduce the cross-sectional area of the flow, but will make the manufacturing simpler (Figure 4a and Figure 4b).

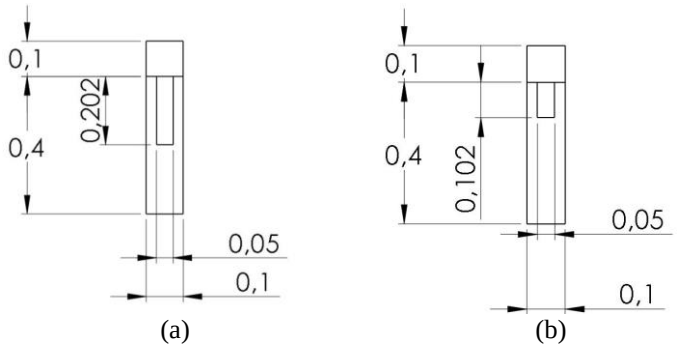

Figure 4. Section of the discrete model of the heatsink with microchannel height of (a) 0.202 mm and (b) 0.102 mm.

Using the same boundary conditions of the experiment, a maximum system temperature of 407 K is achieved for the heatsink with a height of 0.202 mm and 511 K for the heatsink with a height of 0.102 mm - which corresponds to a temperature delta of approximately 111 K and 215 K respectively (Figure 5a and Figure 5b - solid and fluid domains for height of 0.202 mm - and Figure 6a and Figure 6b - solid and fluid domains for height of 0.102 mm). A maximum thermal resistance of 0.140 °C/W is then achieved for the heatsink with the intermediate opening, and of 0.272 °C/W for the heatsink with the smallest opening.

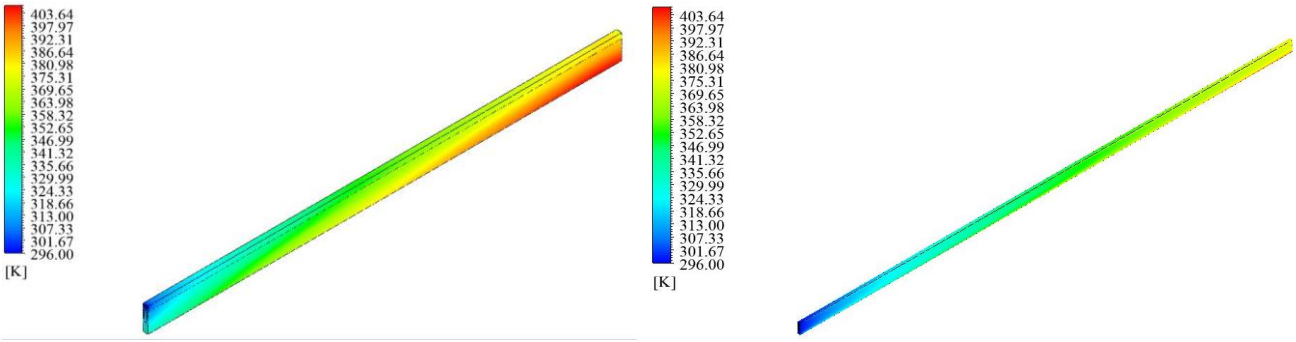

Figure 5. Temperature field of the heatsink with microchannels with a height of 0.202 mm for (a) solid domain and (b) fluid domain.

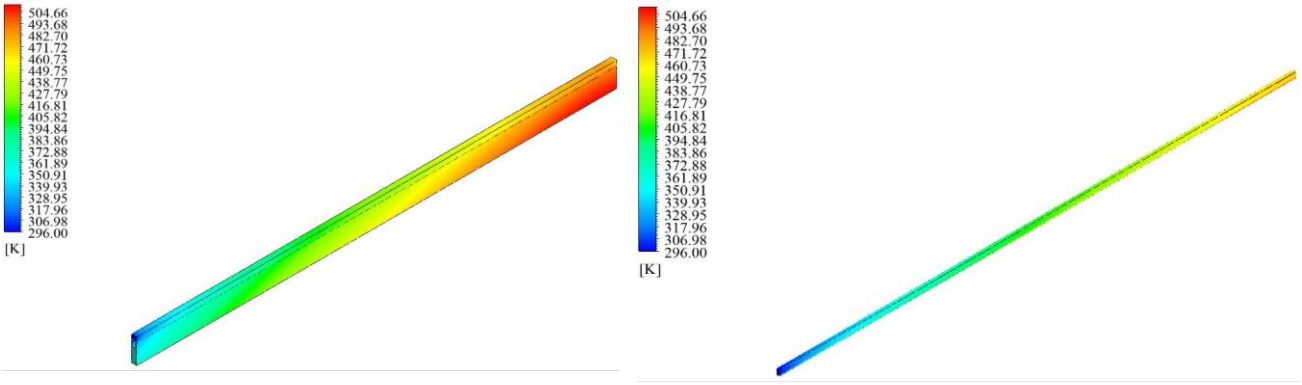

(a) (b)

Figure 6. Temperature field of the heatsink with microchannels with a height of 0.102 mm for (a) solid domain and (b) fluid domain.

The maximum velocities found for the flow of each of the heatsinks are shown in Figure 7a (0.202 mm of depth) and Figure 7b (0.102 mm of depth). The differences found in the velocity fields of the passages with modified geometry were not significant when compared to the velocity found for the original section.

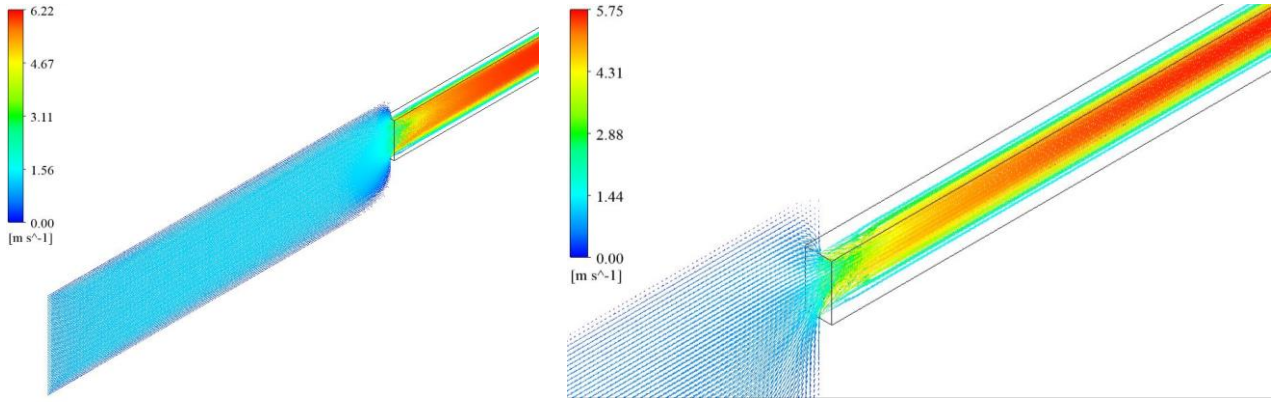

(a) (b)

Figure 7. Velocity vectors in a plane in the central section of the straight microchannel showing the maximum flow velocity for (a) microchannel with a height of 0.202 mm and (b) microchannel with a height of 0.102 mm .

Comparing the results with the original heatsink in a graph (Figure 8) it is possible to perceive the sensitive variation of the thermal resistance with respect to the geometry of the microchannel inlet.

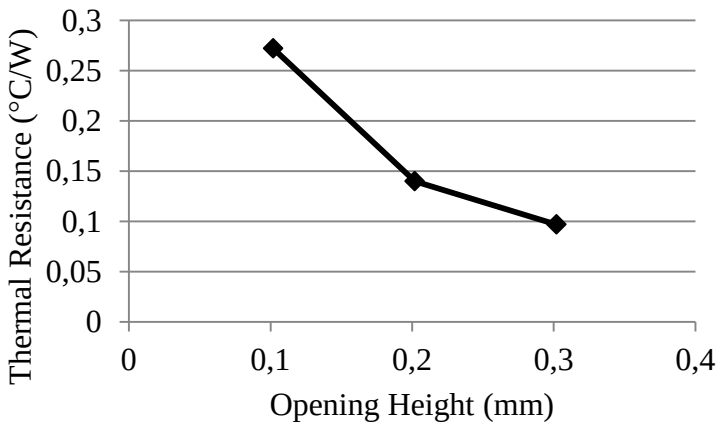

Figure 8. Variation of the height of the opening of the microchannel in relation to the thermal resistance.

3.3.2 Wavy microchannel

Kumar and Zunaid, 2016, presented a numerical analysis of a wavy microchannel with the inclusion of hemispherical obstructions. The main advantages of wavy channels include increasing the surface area for heat flux and a better flow mix, resulting in a better distribution of heat and effective cooling. A model similar to that proposed by the authors was reproduced (Figure 9) using Eq. (2) to model the wave with A = 0.03 mm and λ = 1/2 mm.

$$y = A sen(\frac{2\pi x}{\lambda}) \tag{2}$$

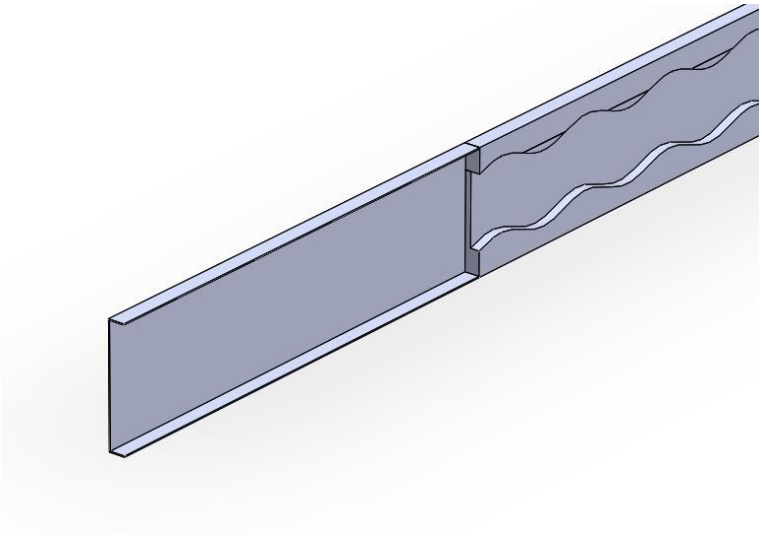

Figure 9. Section of the heat sink with wavy microchannel.

For this case, using the same boundary conditions of the experiment, a maximum system temperature of 376 K is reached, which corresponds to a temperature variation of approximately 80 K (Figure 10a for the solid domain and Figure 10b for the fluid domain) with a thermal resistance of 0.102 °C/W. The maximum flow velocity for this heatsink is shown in Figure 11. The velocity field showed no significant change when compared to the original geometry.

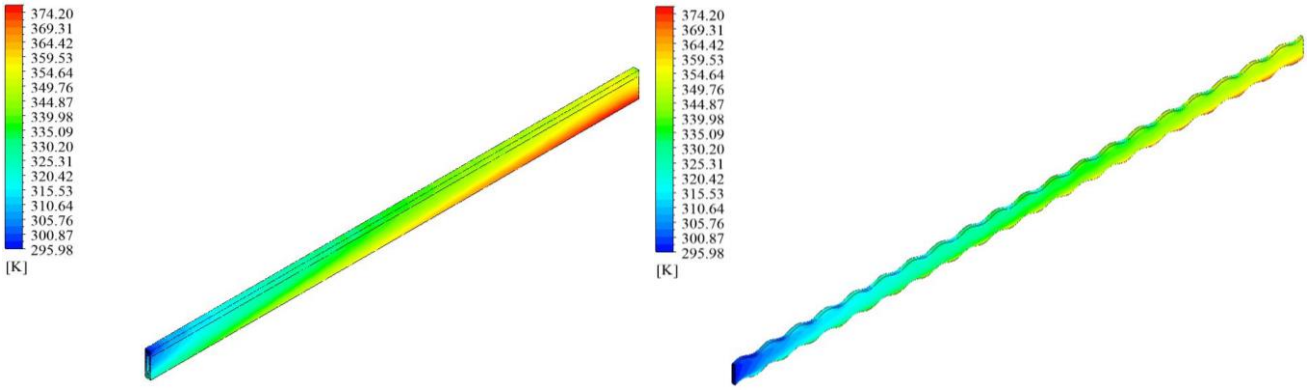

(a) (b)

Figure 10. Heatsink temperature field with water-cooled wavy microchannels at a 0.214 N/mm² pressure and temperature of 273 K at the inlet and power of 790 W/cm² for (a) solid domain and (b) fluid domain.

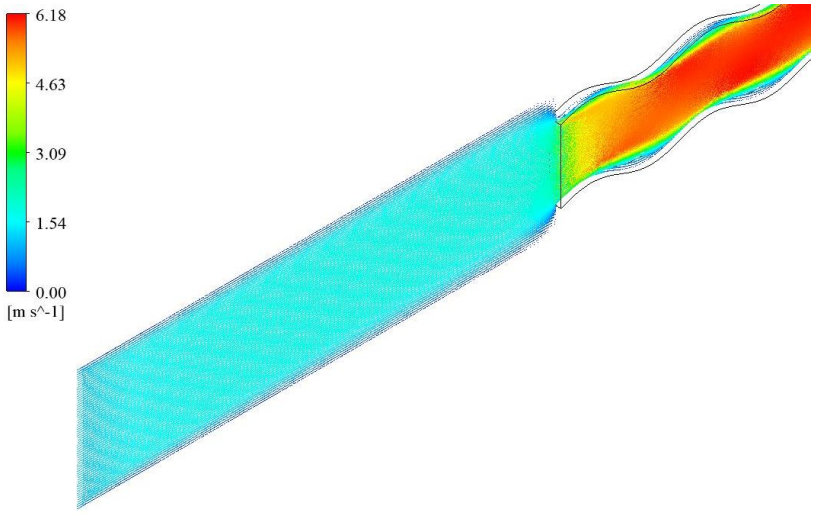

Figure 11. Plane cutting the central section of the wavy microchannel showing the maximum flow velocity.

The maximum thermal resistance found was greater than the heatsink in its original geometry. This can be explained by the fact that the path traveled by the fluid was larger than the path traveled in the straight heatsink and, due to the low Reynolds number imposed by the boundary conditions, the advantages supposedly brought by the heatsink with a wavy microchannel – as better mixture - will only be perceived in much larger Reynolds numbers, where the waves are turbulence promoters, a condition that increases heat transfer.

3.4 Internal and distributed heat generation

A last idealized case where the heat generation was not only generated on a film below the bottom wall of the heatsink but distributed evenly by the silicon volume was simulated. Figure 12 shows the volume at which the heat would be uniformly generated.

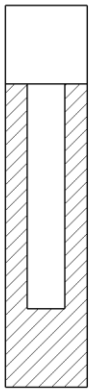

Figure 12. The cross-sectional area represents in a cut where the heat is generated when evenly distributed in the silicon volume.

With a water inlet pressure at 0.214 N/mm² and temperature of 296 K and 790 W/cm² being evenly distributed in the silicon volume, a maximum temperature of 362 K is reached, a temperature variation of 66 K (Figure 13a for the solid domain and Figure 13b for the fluid domain). Thus, using Eq. (1), a thermal resistance of 0.084°C/W is reached.

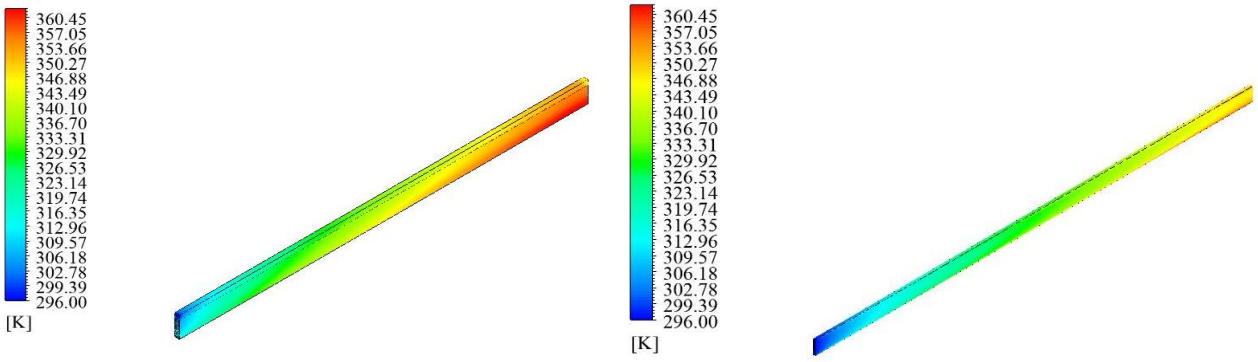

(a) (b)

Figure 13. (a) Heatsink temperature field with a 0.214 N/mm² pressure at the inlet and 296 K temperature and power of 790 W/cm² evenly distributed in the silicon volume (a) solid domain and (b) fluid domain.

The considerable reduction of the thermal resistance demonstrates that the gains in evenly distributed heat in the system are large and that integrated circuit designers should take this fact into account in new designs.

4. CONCLUSIONS

In the present study, numerical tests were carried out involving heatsinks with microchannels. With the results, it was possible to validate the numerical methodology comparing it to experimental results, and to evaluate different methods of improvement. The values obtained and the thermal behaviors of the analyzed heatsinks were in accordance with the literature.

Fluid dynamics results revealed a laminar flow, which is in agreement with the experiment of Tuckerman and Pease, 1981. With 790 W/cm^2 imposed on the bottom of the heatsink, the numerical results of the heat resistance of the heatsink was 0.097 °C/W, while the experimental value was 0.090 °C/W, representing a difference of 7.2%, an excellent agreement when considering factors such as uncertainties of measurement and assumptions induced by the discretization of the heatsink for the numerical analysis.

An analysis was performed simulating the practical effects of integrating the heatsink into a refrigeration system. The results showed that, although the heat resistance of the heatsink was not decreased, the maximum temperature was reduced from 373 K to 350 K, increasing the reliability of the system. Then the heat dissipated was increased to test the limits of this approach (until the temperature was the same as the original system) with up to 1000 W/cm^2 dissipated on the resistor, a result that shows the advantages of a design that ensures a lower inlet temperature.

There were also changes in the geometry of the channel, more specifically in its height, obeying limitations of manufacture, only reducing its opening. The original height of 0.302 mm was first decreased to 0.202 mm and then to 0.102 mm, which increased the pressure drop and hampered the flow of cooling fluid within the channel. The results were within expected range with increase in heatsink heat resistance as the channel area was reduced, ranging from 0.097 °C/W for the original channel to 0.272 °C/W for the lower channel.

A heatsink with wavy microchannels was studied, since these types of channels have the expected advantage of a larger area of contact for the heat flow and a better mixing of the flow. However, the advantages were not observed because with a Reynolds number under the turbulent threshold, mixing effect was not observed, and the waves caused the fluid to travel a greater path inside the channel, thereby heating more than expected. The calculated thermal resistance was 0.102 °C/W.

A last idealized analysis was performed to demonstrate the effect of a better distributed heat flux. The heat flux of 790 W/cm² was uniformly distributed over the silicon volume and the maximum system temperature was reduced to 362 K, reducing the thermal resistance of this system to 0.084 °C/W.

In a comparison with all the results, it is realized that a reduction in the system's inlet temperature along with a better distribution of the heat flux in the chip are able to significantly decrease the maximum temperature of the system, increasing the reliability and the useful life of the system chip into consideration.

5. REFERENCES

Cengel, Y.A., "Heat and Mass Transfer: A Practical Approach", 3. ed.; University of Nevada, Estados Unidos, 2007.

Chein, R. and Chen, J., “Numerical study of the inlet/outlet arrangement effect on microchannel heat sink Performance”. *International Journal of Thermal Sciences* 48, 1627–1638, 2009.

Kandlikar, Satish G., and William J. Grande. "Evolution of Microchannel Flow Passages - Thermohydraulic Performance and Fabrication Technology". *Heat Transfer Engineering*, 24.1, 3-17, 2003.

Kandlikar, S.G. “High Flux Heat Removal With Microchannels: A Roadmap of Challenges and Opportunities”. *ASME 3rd International Conference on Microchannels and Minichannels*, Parts A and B, 59-68, 2005.

Kandlikar, S.G., and Hayner II, Clifford N. “Liquid Cooled Cold Plates for Industrial High-Power Electronic Devices — Thermal Design and Manufacturing Considerations”. *Heat Transfer Engineering*, 30: 12, 918 - 930, 2009.

Kays, W.M. and London, A.L., “Compact Heat Exchangers”, 2nd ed. New York: McGraw-Hill, 1964, p. 14.

Kumar, R. and Zunaid, M., “CFD Analysis of Wavy Microchannel Heat Sink with Hemispherical Obstructions and Comparing it with Experimental Results of Rectangular Microchannel Heat Sink”. *International Journal of Research and Scientific Innovation (IJRSI)*, Issue X, 2016.

Morais, E.L. “Verificação de Soluções Numéricas de Escoamentos Laminares Obtidas com o Método dos Volumes Finitos e Malhas Não-Estruturadas”. Dissertação de Mestrado, UFPR, Curitiba, 2004.

Oliveira, C.P. “Análise do Desempenho de uma Turbina Savonius Helicoidal com Torção de 180° Empregando Simulação Numérica”. Dissertação de Mestrado, PROMEC, UFRGS, Porto Alegre, 2014.

Roache, P. J. “Perspective: A Method for Uniform Reporting of Grid Refinement Studies”, *Journal of Fluids Engineering*, v. 116, p. 405-413, 1994.

Thakre, S.D., Zope, J.P., Bachchuwar, N.A., and Kulkarni, S.S., “Analysis of Straight Microchannel Heatsink Using Computational Fluid Dynamics”. *International Journal of Mechanical Engineering and Technology (IJMET)*, Volume 7, Issue 4, pp 234-242, 2016.

Tuckerman, D.B., and Pease, R.F.W., “High Performance Heatsinking for VLSI”, *IEEE Electron Dev. Let.*, EDL-2, no. 5, pp. 126–129, 1981.

Wallis, G. and Pomerantz, D.I., “Field-Assisted Glass-Metal Sealing”. *Journal of Applied Physics*, vol. 40, no. 10, pp. 3946-3949, 1969.

6. RESPONSIBILITY NOTICE

The authors are the only responsible for the printed material included in this paper.